Phys. Status Solidi B **252,** No. 11, 2407–2411 (2015) / **DOI** 10.1002/pssb.201552226

physica status solidi b
www.pss-b.com
basic solid state physics

Prediction and theoretical investigation of new 2D and 3D periodical structures, having graphene-like bandstructures

A. S. Fedorov[*,1,2], Z. I. Popov[3], A. A. Kuzubov[2], and M. A. Visotin[2]

[1] Kirensky Institute of Physics, Akademgorodok 50, Krasnoyarsk 660036, Russia
[2] Siberian Federal University, av. Svobodny 79, Krasnoyarsk 660041, Russia
[3] National University of Science and Technology MISiS, av. Leninskiy 4, Moscow 119049, Russia

Received 27 April 2015, revised 26 September 2015, accepted 29 September 2015
Published online 26 October 2015

Keywords DFT calculations, Dirac cones, graphene, nanoparticles

[*] Corresponding author: e-mail alex99@iph.krasn.ru, Phone: +7-904-8985175, Fax: +7-391-243-8923

A new family of planar nanostructures having graphene-like electronic band structure is theoretically investigated by density functional theory (DFT). Based on general perturbation theory and a tight-binding model, it was shown that graphene-like planar structures, consisting of identical nanoparticles with relatively weak contacts between them, should have an electronic band structure with Dirac cones. Two such structures, consisting of 71- or 114-silicon atom nanoparticles, were investigated by DFT using VASP software package. The band-structure calculations show the presence of Dirac cones with electron group velocity equal to 1.05×10^5 and 0.53×10^5 m/s, respectively. By generalizing the theory, a new family of 3D structures having intersecting areas with linear dispersion in the band structures was derived. As an example, the band structure of identical 25-atom silicon nanoclusters arranged in a simple cubic lattice was calculated. It was shown that the band structure has features similar to the Dirac cones.

1 Introduction Graphene, since it has been obtained in experiments, has been subject to intense attention [1]. This material is of interest not only because of its potential application in a wide variety of areas, but from a fundamental point of view as well, due to its unique electronic properties. The presence of so-called Dirac cones, i.e., regions with intersecting linear dispersion, in the graphene electronic structure leads to a new relativistic-kind dynamics with its own peculiarities, for example, the Klein paradox [2]. The experimental realization of graphene gave an opportunity to use graphene as a basis for investigations of a new type of particles—massless charged fermions, which do not otherwise occur in nature [2].

However, these particular properties can be reproduced not only in graphene itself or in its recently discovered honeycomb-like symmetry [7–9]; high mobility of a 2D electron gas under honeycomb external potential [10–13], and honeycomb superlattices of molecules and nanoparticles [14, 15]. It is common for these cases that interactions inside individual particles, forming the graphene-like lattice, or regions of space with large external potential is substantially greater than the interaction between the particles or regions of space. This condition

2 Theory and methods

2.1 Theoretical foundation To prove that the band structure of a periodic structure formed from weakly contacting equivalent nanoparticles may have Dirac cones, we present here two theoretical justifications.

Suppose that there are isolated identical nanoparticles of a nearly spherical shape. We can also assume that some electrons in the nanoparticle, which are close to the Fermi level, would have spherically shaped wave functions $\phi_{\text{isolated}}(\mathbf{r})$. To find an electronic band structure of such periodic lattice, the standard perturbation theory (PT) for a degenerate case can be used, assuming that the interaction and overlapping of the individual particles electronic wavefunctions is weak. One can use the Bloch theorem:

$$\psi_{\text{k}}(\mathbf{r}) = \frac{1}{N_{\text{cells}}} \sum_{\mathbf{l}=1}^{N_{\text{cells}}} e^{i\mathbf{kl}} \phi_{\text{isolated}}(\mathbf{r}-\mathbf{l}). \tag{1}$$

For simplicity, we assume that the graphene-like honeycomb hexagonal lattice is built from identical nanoparticles. So, the unit cell vectors are

$$\mathbf{a}_1 = \frac{a}{2}\left(3,\sqrt{3}\right);\ \ \mathbf{a}_2 = \frac{a}{2}\left(3,-\sqrt{3}\right), \tag{2}$$

where a is the interparticle distance. The corresponding reciprocal lattice vectors $\mathbf{b}_1$ and $\mathbf{b}_2$, defined by the condition $\mathbf{a}_i\mathbf{b}_j = 2\pi\delta_{ij}$ are then

$$\mathbf{b}_1 = \frac{2\pi}{3a}\left(1,\sqrt{3}\right);\ \ \mathbf{b}_2 = \frac{2\pi}{3a}\left(1,-\sqrt{3}\right). \tag{3}$$

The first Brillouin zone (FBZ) of the hexagonal reciprocal lattice has six points at the corners (Dirac points), separated into two inequivalent groups, labeled $\mathbf{K}$ and $\mathbf{K}'$, having coordinates

$$\mathbf{K} = \frac{2\pi}{3a}\left(1,\frac{1}{\sqrt{3}}\right);\ \ \mathbf{K}' = \frac{2\pi}{3a}\left(1,-\frac{1}{\sqrt{3}}\right). \tag{4}$$

It is easy to show that $1 + e^{i\mathbf{Ka}_1} + e^{i\mathbf{Ka}_2} = 0$ for both Dirac points.

Taking into account that the equivalent nanoparticles interaction is weak, PT for a degenerate case leads to the secular equation

$$\det\begin{pmatrix} V_{11}-\Delta E & V_{12}(1+e^{i\mathbf{ka}_1}+e^{i\mathbf{ka}_2}) \\ V_{21}(1+e^{-i\mathbf{ka}_1}+e^{-i\mathbf{ka}_2}) & V_{22}-\Delta E \end{pmatrix} = 0. \tag{5}$$

Here, $V_{11} = V_{22} = \langle\phi_{\text{isolated}}(\mathbf{r})|\Delta U(\mathbf{r})|\phi_{\text{isolated}}(\mathbf{r})\rangle$ is the nanoparticle energy levels shift due to an interaction potential $\Delta U(\mathbf{r}) = U(\mathbf{r}) - U_{\text{isolated}}(\mathbf{r})$ acting between nearest nanoparticles, where $\phi_{\text{isolated}}(\mathbf{r})$ is the corresponding nanoparticle wave function, $V_{12} = V_{21}^* = \langle\phi_{\text{isolated}}(\mathbf{r})|\Delta U(\mathbf{r})|\phi_{\text{isolated}}(\mathbf{r}-\mathbf{l})\rangle$ is the matrix element of interaction $\Delta U(\mathbf{r})$ between particles, where $\mathbf{l}$ defines the vectors connecting nearest particles, and ΔE is the first-order energy correction due to the interaction between nanoparticles.

The factor $(1 + e^{i\mathbf{ka}_1} + e^{i\mathbf{ka}_2})$ is responsible for the interaction of the nanoparticle with its neighbors in the same and in two neighboring unit cells. Calculating the determinant (5), it is easy to find an expression for the energy correction, which is linear in $\mathbf{k}$ wave vector near the Dirac points

$$\Delta E(\mathbf{k}) = V_{11} \pm |V_{12}|\left|1 + e^{i\mathbf{ka}_1} + e^{i\mathbf{ka}_2}\right|. \tag{6}$$

In accordance with the above expression, for the case $\mathbf{k} = \mathbf{K}$ or $\mathbf{K}'$ Dirac points, the energy correction $\Delta E(\mathbf{k})$=0, but for small deviations from these points the factor $\left|1 + e^{i\mathbf{ka}} + e^{i\mathbf{kb}}\right|$ will be linear in relation to the $|\mathbf{k}-\mathbf{K}|$ or $|\mathbf{k}-\mathbf{K}'|$ which explains the Dirac cones appearance in these points.

The same result can be obtained easily with help of a tight-binding model, where the total band electron energy $E(\mathbf{k})$ is calculated using a variational equation

$$E(\mathbf{k}) = \frac{\int \psi_k^*(\mathbf{r})\left\{-\frac{\hbar^2}{2m}\nabla^2 + U(\mathbf{r})\right\}\psi_k(\mathbf{r})\mathrm{d}^3\mathbf{r}}{\int \psi_k^*(\mathbf{r})\psi_k(\mathbf{r})\mathrm{d}^3 r}. \tag{7}$$

Assuming that the nanoparticles wave functions are weakly overlapped for nearest particles only, Eqs. (1) and (7) lead to

$$E(\mathbf{k}) \approx E_{\text{isolated}} + \Delta E;\ \ \Delta E = -\sum_l \varepsilon(\mathbf{l}) e^{i\mathbf{kl}}, \tag{8}$$

$$\varepsilon(\mathbf{l}) = -\int \phi_{\text{isolated}}^*(\mathbf{r}+\mathbf{l})\Delta U(\mathbf{r})\phi_{\text{isolated}}(\mathbf{r})\mathrm{d}^3\mathbf{r}. \tag{9}$$

For identical particles of a nearly spherical shape and that are equidistant from each other $\varepsilon(\mathbf{l}) \approx$ const, so Dirac cones will be also observed in the $\mathbf{K}$ and $\mathbf{K}'$ points, where

$$\sum_{\mathbf{l}} e^{i\mathbf{kl}} = 0 \tag{10}$$

is satisfied in analogy to Eq. (6). In this work we have investigated some lattices that consist of weakly interacting nanoparticles, looking for Dirac cones, whose general condition is the fulfillment of Eq. (10).

2.2 Computational details All calculations of geometrical and electronic structures were conducted using VASP 5.3 (Vienna ab-initio simulation package) package [16–18] within the framework of DFT method [19, 20] in the plane wave basis set. The projector augmented wave (PAW) method [21, 22] and the general gradient

approximation (GGA) in the Perdew–Burke–Ernzerhof (PBE) form [23] were used in all calculations.

To determine whether the aggregation of the nanoparticles into a periodic lattice is energetically allowed, the total energy of separated nanoparticles was calculated as well. Having the energy of free-standing particles, the lattice binding energy is calculated as:

$$E_{\text{bind}} = E_{\text{lat}} - 2E_{\text{single}}, \tag{11}$$

where E_{bind} is the binding energy per unit cell, E_{lat} is the total energy of the unit cell, and E_{single} is the total energy of a free-standing nanoparticle having relaxed structure.

3 Results and discussion

3.1 Planar honeycomb lattices First, silicon nanoparticles arranged in the 2D honeycomb lattice were modeled. It is generally known that in the diamond-like silicon lattice the [111] direction has an axis of symmetry of order 3. So, if a honeycomb-like lattice is build up from a crystal in a plane perpendicular to this axis, the atoms and bonds would have the same symmetry axis. Separate nanoparticles of two different sizes were obtained by cutting out nearly spherical regions from the silicon lattice and removing single-bonded atoms from the nanoparticle surface. In doing so, the symmetry of third order remained in the nanoparticles. It seems that the merging of these nanoparticles into a planar lattice having the third-order axis of symmetry, using—for example—an inert substrate surface, can result in a graphene-like lattice formation composed of these particles.

To do this, two kinds of nanoparticles were used. In one case the nanoparticle contained 71 atoms, while its diameter was equal to 14.5 Å; in another, the nanoparticle has 114 atoms and a diameter of 18.3 Å, see Fig. 1. A full optimization of the nanoparticle geometries were carried out with the help of DFT calculations for both types of nanoparticles.

To make the 2D graphene-like lattices (Fig. 2), consisting of these nanoparticles, a unit cell with periodic boundary conditions was built. It was sized according to (2) and contained two particles described above. Then, the unit

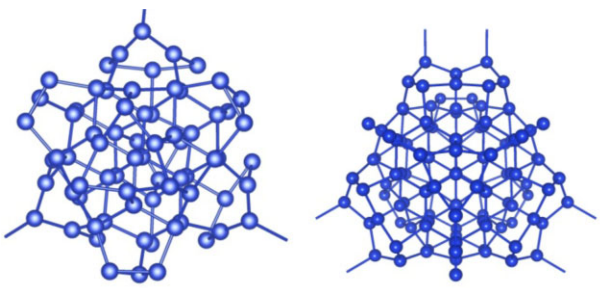

Figure 1 The structure of silicon nanoparticle containing 71 (left panel) and 114 (right panel) atoms. The dangling bonds show the bonds formed between the particles when the honeycomb superlattice is formed.

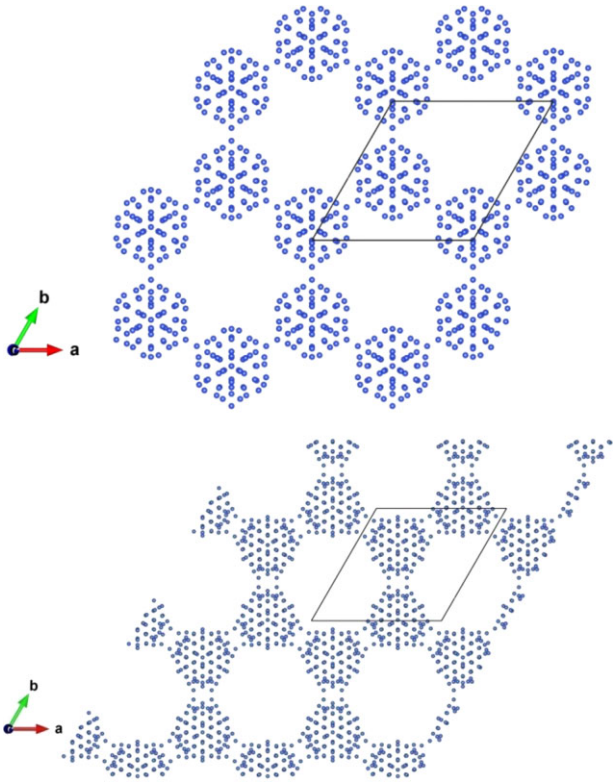

Figure 2 The honeycomb lattices of silicon nanoparticles containing 71 and 114 atoms. Bold lines show the unit cells.

cell height a_3 in the direction perpendicular to the honeycomb lattice plane was set to 30 Å, which resulted in at least 13 Å of vacuum spacing between periodic images of the graphene-like layers. This guaranteed the absence of interactions between them.

Then, the lattice geometrical optimization was made with respect to all atomic coordinates, until the maximal force acting on all atoms was less than 0.1 eV/Å and with respect to cell parameters, until the pressure in the plane was less than 1 kbar. Both optimized geometries are listed in the Supporting Information. For calculating integrals over the first Brillouin zone (1 BZ), the Monkhorst–Pack scheme [24] with improved tetrahedron method [25] was used. Mesh sizes of $5 \times 5 \times 1$ points, in the case of 71 atoms, and $3 \times 3 \times 1$ points, in the case of 114 atoms, were sufficient for full energy convergence within 0.01 eV. The cutoff energy for the plane wave basis, E_{cutoff} was taken to be 245.3 eV. After the structure optimization, the density of states (DOS) and the band structure $E(k)$ along Γ–K and K–M high-symmetry directions were calculated for both types of structures, see Figs. 3 and 4.

For the structure consisting of 114 atoms nanoparticles the DOS pits at the Dirac cones (K points) are in good agreement with the positions of some DOS peaks of the isolated nanoparticle, corresponding to the particle local levels, see Supporting Information, but that are not shown here for the sake of simplicity. This is fully explained by the

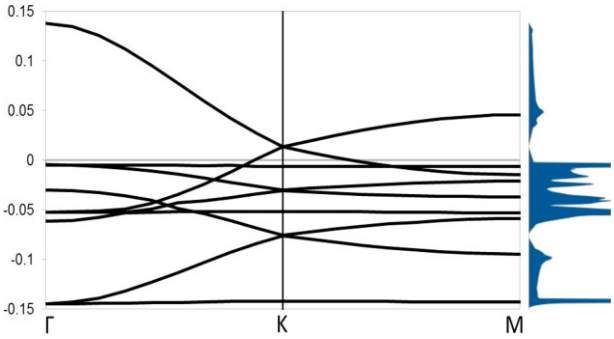

Figure 3 Band structure and DOS of the honeycomb lattice consisting of 71-atom silicon nanoparticles. 0 corresponds to the Fermi level. Energy units are in eV.

formula (6), where the energy of the cone centers is defined by the isolated particle local levels.

For isolated particles of 71 atoms the DOS peak positions are not coincident (bias is ~0.1 eV) with the Dirac cone positions. It can be explained by the substantially greater interparticle interactions compared to intraparticle interactions and relatively large overlap of the wave functions of individual particles in comparison with the case of a 114-atom particles, where the particles contacts are relatively much weaker and formula (6) performed with greater accuracy.

Based on the resulting dispersion law, the derivative dE/dk was found in the vicinity of the Dirac cone (K point), to determine the group velocity of electrons according to the formula

$$v_{\text{Fermi}} = \frac{1}{\hbar}\frac{dE}{dk}. \tag{12}$$

Figures 1 and 2 show the structures of nanoparticles and the lattices they build up.

Using (11), the binding energies of the lattices consisting of fully relaxed nanoparticles containing 71 or114 atoms were calculated. They were equal to –7.39 and –12.27 eV,

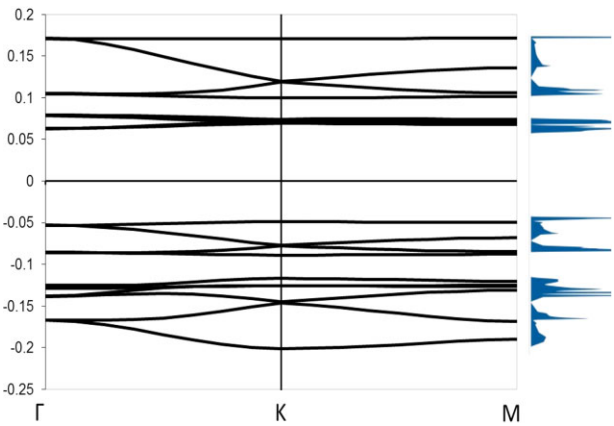

Figure 4 Band structure and DOS of the honeycomb lattice consisting of 114-atom silicon nanoparticles. 0 corresponds to the Fermi level. Energy units are in eV.

respectively. These high values indicated that during coagulation of the particles with relaxed surface they formed multiple chemical bonds between themselves. Moreover, the energies per atom in the resulting structures were –4.75 and –4.80 eV, which is rather comparable to the cohesive energy of silicon structure equal to –5.39 eV/atom according to our calculations. The band structures of the lattices (Figs. 3 and 4) showed several Dirac cones at the K points above and below the Fermi level. The group velocities, calculated for the cones, which are the closest to the Fermi level, were equal to: for the lattice of 71-atom nanoparticles—1.05×10^5 m/s; for 114-atom particles—0.53×10^5 m/s. These values are by one order of magnitude less than the values for graphene ($\approx 1 \times 10^6$ m/s [3]) and silicene (5.31×10^5 m/s [26]).

3.2 3D cubic superlattices In the second part of this work, geometrical and electronic structure of a three-dimensional cubic superlattice, containing 25-atom silicon nanoclusters were calculated. Every cluster had six nearest-neighbor equivalent clusters. To comply with cubic symmetry of the lattice, the nanoclusters were taken in the form of octahedra, where all atoms, except for some of them on the nanocluster surface, were sixfold coordinated. This cluster shape was used to easily create symmetrical contacts between clusters, which was desirable to confirm our approach. The discrepancy in the coordination number (6) and the normal value (4) is possible, as in some studies [27] it was shown that small stable silicon clusters may have a significant number of atoms with coordination number different from 4.

The value (–3.99 eV/atom) of the binding energy of these relaxed octahedron clusters was close to the value (–3.92 eV/atom) of the most stable clusters, defined by similar DFT-GGA calculations [27].

First, the geometrical structure of a free-standing cluster was optimized, then the clusters were combined into a periodic lattice, and the whole structure was optimized once again, see Supporting Information. The lattice parameter was found to be 11.55 Å. Then, the band structure was obtained.

Following Eq. (10) for the Dirac cones appearance, the band structure was analyzed in the vicinity of a two-dimensional surface, that can be found as

$$\begin{aligned}&\cos\pi(k_x + k_y - k_z) + \cos\pi(k_x - k_y + k_z)\\ &\quad + \cos\pi(k_x - k_y - k_z) = 0,\end{aligned} \tag{13}$$

where k_x, k_y, k_z are the wave vector coordinates in the reciprocal space. As a result of cluster aggregation, we observed that the lowest valence energy level had been split into two bands intersecting on this surface.

In the surface vicinity, a one-dimensional analog of the Dirac cone can be found for different directions. Figure 5 shows the electronic dispersion along the Γ–C direction, where the point C having coordinates {1/3; 1/3; 2/3}, belongs to the intersection surface and satisfies Eqs. (10) and

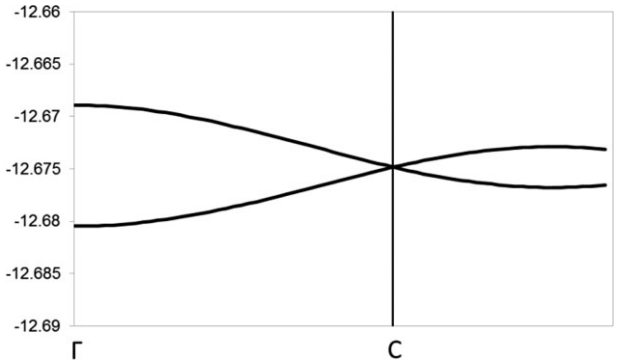

Figure 5 The lowest-energy valence level in the band structure of the simple cubic lattice consisting of 25-atom silicon nanoclusters. Energy units are in eV.

(13). It could be observed that the intersection of two zones occurs at this point. Because of the very small zones dispersion (~ 0.01 eV) it was difficult to build a correct DOS for this energy range, so the DOS is not shown there. An absence of other zones intersections along the Γ–C direction can be explained by a significant overlap of wavefunctions corresponding to the nanocluster high energy levels, which does not allow using the perturbation theory (formula (6)).

Using Eq. (12), the group velocity was estimated to be 4.5×10^3 m/s for this 3D case.

4 Conclusions It is shown that the presence of Dirac cones in the band structure is a common case for structures where Eq. (10) is fulfilled, in particular for the planar honeycomb structure built of small silicon nanoparticles. It is also demonstrated that Dirac cones for different directions can be found in three-dimensional structures, for example, in the simple cubic structure constructed from identical silicon nanoparticles.

Supporting Information

Additional supporting information may be found in the online version of this article at the publisher's web-site.

Acknowledgements This work was supported by the Ministry of Education and Science of Russia (Russian–Japanese joined project, Agreement No. 14.613.21.0010, ID RFMEFI61314 × 0010). The authors are grateful to the Joint Supercomputer Center of Russian Academy of Sciences, Moscow and Siberian Supercomputer Center (SSCC) of SB RAS, Novosibirsk for the opportunity of using their computer clusters to perform the calculations.

References

[1] K. S. Novoselov, A. K. Geim, and S. V. Morozov, Science **306**, 666 (2004).
[2] M. I. Katsnelson, K. S. Novoselov, and A. K. Geim, Nature Phys. **2**, 620 (2006).
[3] B. Aufray, A. Kara, S. Vizzini, and H. Oughaddou, Appl. Phys. Lett. **96**, 183102 (2010).
[4] M. Polini, F. Guinea, and M. Lewenstein, Nature Nanotechnol. **8**, 625 (2013).
[5] B. Wunsch, F. Guinea, and F. Sols, New J. Phys. **10**, 103027 (2008).
[6] L. Tarruell, D. Greif, and T. Uehlinger, Nature **483**, 302 (2012).
[7] F. D. M. Haldane and S. Raghu, Phys. Rev. Lett. **100**, 013904 (2008).
[8] R. A. Sepkhanov, Y. B. Bazaliy, and C. W. J. Beenakker, Phys. Rev. A **75**, (2007).
[9] O. Peleg, G. Bartal, and B. Freedman, Phys. Rev. Lett. **98**, 103901 (2007).
[10] C. H. Park, L. Yang, and Y. W. Son, Phys. Rev. Lett. **101**, 126804 (2008).
[11] C. H. Park and S. G. Louie, Nano Lett. **9**, 1793 (2009).
[12] M. Gibertini, A. Singha, and V. Pellegrini, Phys. Rev. B **79**, (2009).
[13] S. Goswami, M. A. Aamir, and C. Siegert, Phys. Rev. B **85**, 075427 (2012).
[14] K. K. Gomes, W. Mar, and W. Ko, Nature **483**, 306 (2012).
[15] E. Kalesaki, C. Delerue, and C. M. Smith, Phys. Rev. X **4**, (2014).
[16] G. Kresse and J. Hafner, Phys. Rev. B **47**, 558 (1993).
[17] G. Kresse and J. Hafner, Phys. Rev. B **49**, 14251 (1994).
[18] G. Kresse and J. Furthmüller, Phys. Rev. B **54**, 11169 (1996).
[19] P. Hohenberg and W. Kohn, Phys. Rev. **136**, B864 (1964).
[20] W. Kohn and L. J. Sham, Phys. Rev. **140**, A1133 (1695).
[21] J. P. Perdew, K. Burke, and M. Ernzerhof, Phys. Rev. B **77**, 3865 (1996).
[22] P. E. Blöchl, Phys. Rev. B **50**, 17953 (1994).
[23] G. Kresse, and D. Joubert, Phys. Rev. B **59**, 1758 (1999).
[24] H. J. Monkhorst, and J. D. Pack, Phys. Rev. B **13**, 5188 (1976).
[25] P. E. Blöchl, O. Jepsen, and O. K. Andersen, Phys. Rev. B **49**, 16223 (1994).
[26] N. D. Drummond and V. Zólyomi, and V. I. Fal'ko, Phys. Rev. B **85**, 075423 (2012).
[27] A. Sieck, T. Frauenheim, and K. A. Jackson, Phys. Status Solidi B **240** (3), 537–548 (2003).